

Reconstruction of a near-surface tornado wind field from observed building damage

Jianjun Luo^{*1,2}, Daan Liang^{1a} and Christopher Weiss^{1b}

¹National Wind Institute, Texas Tech University, 2500 Broadway, Lubbock, TX 79409, USA

²AIR Worldwide, 131 Dartmouth Street, Boston, MA 02116, USA

(Received May 16, 2014, Revised November 12, 2014, Accepted January 21, 2015)

Abstract. In this study, residential building damage states observed from a post-tornado damage survey in Joplin after a 2011 EF 5 tornado were used to reconstruct the near-surface wind field. It was based on well-studied relationships between Degrees of Damage (DOD) of building and wind speeds in the Enhanced Fujita (EF) scale. A total of 4,166 one- or two-family residences (FR12) located in the study area were selected and their DODs were recorded. Then, the wind speeds were estimated with the EF scale. The peak wind speed profile estimated from damage of buildings was used to fit a translating analytical vortex model. Agreement between simulated peak wind speeds and observed damages confirms the feasibility of using post-tornado damage surveys for reconstructing the near-surface wind field. In addition to peak wind speeds, the model can create the time history of wind speed and direction at any given point, offering opportunity to better understand tornado parameters and wind field structures. Future work could extend the method to tornadoes of different characteristics and therefore improve model's generalizability.

Keywords: tornadoes; near-surface wind field; Rankine vortex model; Enhanced Fujita scale; degree of damage; post-tornado damage survey; residential buildings

1. Introduction

Characterization and quantification of near-surface wind fields of tornadoes are important for risk analysis, structural design, and public safety as wind speeds vary significantly in both spatial and time domains. Lack of sufficient direct observations continues to persist as tornadoes are relatively rare, short-lived, small in coverage area, difficult to forecast, and often possess violent destructive forces (Mehta 2013, Wurman *et al.* 2013). To overcome these challenges, a somewhat idealized process is often adopted for modelling tornado wind field (Davies-Jones *et al.* 2001, Doswell III and Burgess 1993, Lewellen and Lewellen 2007).

There are three general categories of methods employed to model tornado structures, i.e., theoretical, experimental, and empirical methods. Theoretical methods use mathematical representations of physical relationships to describe the vortex structure as derived from Navier-Stokes equations. With results from tornado generators, experimental methods transfer

*Corresponding author, Ph.D., E-mail: jluo@air-worldwide.com

^a Associate Professor, E-mail: daan.liang@ttu.edu

^b Associate Professor, E-mail: chris.weiss@ttu.edu

uncontrolled phenomena into controllable laboratory models to attain a better understanding of the dynamics of flow structures and wind fields. In comparison, empirical methods create tornado wind fields based on in situ measurement, radar observations, or post-storm damage survey.

Integrating theoretical and empirical methods, this study is aimed at reconstructing a near-surface wind field by fitting a simplified translating analytical vortex model with post-tornado damage survey data collected from Joplin, MO tornado of 2011. It makes the use of well-studied relationships between degrees of damage of buildings and wind speeds in the Enhanced Fujita (EF) scale. Furthermore, wind field parameters are estimated from statistical methods rather than subjective evaluations, which usually suffer from human biases, allowing the new method to be applied to and replicated in other events. Since the major objective of this study is to develop a robust method for using post-tornado damage surveys to reconstruct near-surface wind field, only a section of an EF 5 tornado with relatively homogenous characteristics was examined. Future studies could extend to tornadoes with varied attributes.

The remaining of the paper is organized as follows: Section 1 reviews previous literature on tornado vortex models, past efforts in tornado observation, and various wind field modeling methods. Section 2 introduces the methodology, datasets, and statistical methods. The results of this study are presented in Section 3 and discussed in Section 4. Finally, Section 5 includes conclusions and comments on future work.

1.1 Tornado vortex model

For engineering applications, the Rankine vortex model and many of its variants are frequently used to characterize tornado structures. The Rankine vortex model assumes radial symmetry for a steady vortex in a viscous fluid (Rankine 1882). Under a cylindrical coordinate system (r, θ, z), the vortex is divided into two regions: a forced vortex in its central core with tangential velocity linearly proportional to the radial distance and a free vortex surrounded the core with tangential velocity inversely proportional to the radial distance. The maximal tangential velocity appears on the interface of those two. The other velocity components (radial and vertical) are set identically to zero. The formulas for the velocity components of any point from the radial distance r to the vortex center are given by

$$V_r = 0 \quad (1)$$

$$V_t = V_{tmax} \frac{r}{R_{tmax}} \quad \text{when } 0 \leq r \leq R_{tmax} \quad (2)$$

$$V_t = V_{tmax} \frac{R_{tmax}}{r} \quad \text{when } r > R_{tmax} \quad (3)$$

$$V_z = 0 \quad (4)$$

where V_r is the radial wind velocity, V_z is the vertical wind velocity, V_t is the tangential wind velocity, V_{tmax} is the maximum tangential wind velocity, r is the radial distance from the vortex center, and R_{tmax} is radius of the maximum tangential wind velocity.

Since the Rankine vortex model considers only the circumferential component of wind velocity, Letzmann, as well as other researchers (e.g., Zrnice *et al.*, Brown and Wood, Potvin *et al.*) extended this model by describing the axisymmetric radial flow in the same way as it did for axisymmetric tangential flow to model the divergent/convergent areas of the horizontal flow field (Brown and Wood 1991, Peterson 1992, Potvin *et al.* 2009, Zrnice *et al.* 1985), as shown in the Eqs. (5) and (6).

$$V_r = V_{rmax} \frac{r}{R_{rmax}} \quad \text{when } 0 \leq r \leq R_{rmax} \quad (5)$$

$$V_r = V_{rmax} \frac{R_{rmax}}{r} \quad \text{when } r > R_{rmax} \quad (6)$$

where V_{rmax} is defined as the maximum radial velocity at its core radius R_{rmax} .

The combined velocity profile of a more generalized Rankine vortex model can be given by

$$V_r = V_{rmax} \frac{r}{R_{rmax}} \quad \text{when } 0 \leq r \leq R_{rmax} \quad (7)$$

$$V_r = V_{rmax} \left(\frac{R_{rmax}}{r}\right)^\beta \quad \text{when } r > R_{rmax} \quad (8)$$

$$V_t = V_{tmax} \frac{r}{R_{tmax}} \quad \text{when } 0 \leq r \leq R_{tmax} \quad (9)$$

$$V_t = V_{tmax} \left(\frac{R_{tmax}}{r}\right)^\beta \quad \text{when } r > R_{tmax} \quad (10)$$

$$V_z = 0 \quad (11)$$

where β is the decay coefficient. The earlier Rankine model is a special case of this model where $\beta=1$.

In reality, the angular momentum outside the core radius is unlikely to be constant and then β could be a number other than 1. According to the field measurement, β might be around 0.5 - 0.8, or even 0.2 - 0.6 in some cases (Kosiba and Wurman 2010, Kosiba *et al.* 2008, Mallen *et al.* 2005, Wurman and Alexander 2005, Wurman and Gill 2000).

Moreover, researchers have modified the original Rankine vortex model by altering assumptions or constraints on parameters. For example, the Burgers-Rott vortex model addressed the unrealistic assumption of zero values for vertical and radial components of wind velocity in the Rankine vortex model and reflected the effect of eddy viscosity. Hence tangential velocity has a rounded maximum at the core radius rather than cusp at its core radius as in the Rankine model (Burgers 1948, Rott 1958). Thus, the Burgers-Rott model is deemed more realistic (Wood and Brown 2011).The Sullivan vortex model is a more complex model and can capture phenomenon such as the two-celled vortex, which could not be explained by the previous two models (Sullivan 1959). More recently, Wood and White (2011) presented a new parametric model by including five key parameters in the tangential velocity profile: maximum tangential wind, radius of maximum tangential wind, and three power-law exponents that shape different parts of the wind speed profile. Nevertheless, the Rankine vortex model is easy to implement and thus has been frequently adopted by engineering applications in spite of its over-simplification of the dynamics.

1.2 Empirical models and post-tornado damage survey

Empirical models are based on observations, which could come from in situ measurement, Doppler radar and post-tornado damage survey. The closer the instruments are located to tornado, the better the measurements are to describe the temporally and spatially variances among the tangential, vertical and radial wind components as well as the translation speed of the tornado. However, reliable in situ measurement of the wind near the ground is extremely difficult to obtain because of risks presented by intense winds and striking debris (Karstens *et al.* 2010, Wurman *et al.* 2013). Thus, the majority of empirical models are based on radar observations and post-storm

damage surveys.

The use of radars in observing tornadoes dates back to 1950s as an effective and safe way for wind data collection. At its early stage, researchers used traditional stationary meteorological radars to discover tornado structures and estimate wind speeds. However, the limitations of the fixed-location meteorological radars are noticeable. Most tornadoes occur far away from stations and thus are hard to measure as radar beams spread and deviate from the surface of the earth. Moreover, the spatial resolution of the traditional Doppler radar is too low to resolve uniquely the different portions of the tornado flow, and the temporal resolution restricted by scanning strategies of the radar is too limited to sample physical processes over the timescale of seconds to minutes (Davies-Jones *et al.* 2001, Wurman *et al.* 2010, 1997).

To obtain high resolution observations of tornado vortices, Bluestein *et al.* (1995) installed a mobile 3-mm-wavelength pulsed Doppler radar on a van and observed severe convective storms in the Southern Plains during 1993 and 1994, while Wurman (1997) constructed a portable, pencil-beam, pulsed, 3-cm wavelength Doppler radar called the Doppler on Wheels (DOW) and successfully measured several tornadoes. With those high resolution mobile radar systems, a large volume of data have been collected and the understanding of the tornado wind field has been enriched (e.g., Bluestein *et al.* 2003, Burgess *et al.* 2002, Kosiba and Wurman 2010, Kosiba *et al.* 2008, Lee and Wurman 2005, Tanamachi *et al.* 2007, Wurman and Alexander 2005, Wurman and Gill 2000). Furthermore, comparing the DOW measurements with corresponding WSR-88D measurement, Toth *et al.* (2013) developed a linear regression model to estimate the low level tornadic wind speeds from WSR-88D.

However, mobile Doppler radar generally cannot measure speeds of wind lower than 20 - 30 m above ground level (AGL) because of ground clutter contamination (Lewellen and Zimmerman 2008, Wurman *et al.* 2007). To solve this problem, Wurman *et al.* examined the relationship of tornado winds above and below 30 m AGL by combining in situ measurements and DOW measurements from several cases (Wurman *et al.* 2013, 2007). From that, Wurman *et al.* (2007) further developed a Rankine vortex-based axisymmetric wind field model constrained by DOW data and estimated damage of several major cities from simulated tornadoes.

According to Doswell III *et al.* (2009), only about 20 tornadoes have been observed every year by mobile Doppler radar compared to over 1,000 tornado occurrences in the United States. It is due to the unpredictable nature of tornadoes and relative limited resources available. Moreover, for hazard analysis, tornado intensity at the ground level is essential because typical residential buildings are below 30 m AGL where even mobile Doppler radar cannot sense with ground contamination.

Since damage from the tornado has a strong correlation with wind speed, post-tornado damage surveys have been proposed to infer the near-surface tornado wind field. For example, researchers have reconstructed the wind field from forest damage by matching observed tree damage patterns with simulated tree damage patterns (Bech *et al.* 2009, Beck and Dotzek 2010, Holland *et al.* 2006, Karstens *et al.* 2013, NIST 2013). Their work usually includes three key parts: a translating Rankine vortex model, tree fall model, and forest damage pattern. Similarly, damage patterns of buildings contain useful information and can be used to reconstruct near-surface wind fields.

However, a residential building, a very common damage indicator in Enhanced Fujita scale (EF scale) and a type of building that receives most attention from academia and industry, has rarely been used to reconstruct wind field. The idea to estimate wind speed in a tornado from the damage of buildings was proposed by Fujita who developed the Fujita scale (F scale) to classify the tornado intensity (Fujita 1981, 1971). To overcome the problems associated with F scale, such as a

shortage of damage indicators, ignorance of construction quality and variability, and overestimates of wind speeds, the EF scale was adopted for damage survey in 2007. The EF scale has 28 damage indicators (DIs) and corresponding degrees of damage (DODs) (WISE 2006). For each DOD, it lists the wind speeds that could cause the damage, which include expected wind speed, lower bound wind speed, and upper bound wind speed. During a tornado, each damage indicator can act like an anemometer that records the wind speeds it experienced. After collecting a large amount of DIs in different locations within a tornado swath from the post-tornado damage survey and estimating the wind speeds based on EF scale, the wind field can be reconstructed.

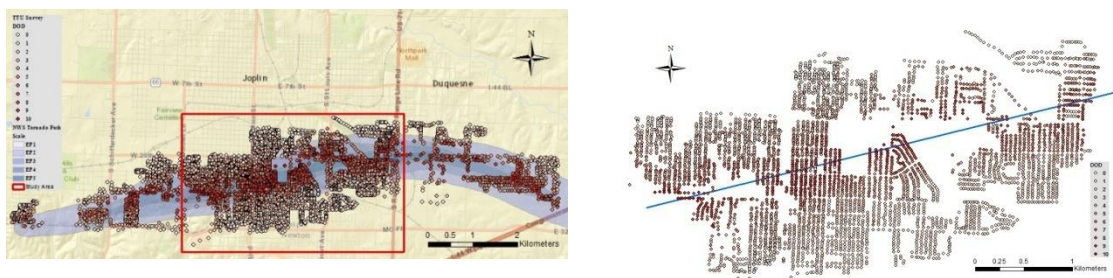
As there was no direct near-surface wind speed measurement available during the Joplin Tornado (NIST 2013), this study investigates the damage pattern of residential buildings from the post-tornado damage survey and rebuilds the near-surface wind environment. The results are compared to those of other studies that have utilized forest damage pattern analysis on the same area.

2. Methodology

2.1 Data collection and processing

On May 22, 2011, an EF 5 tornado occurred in Joplin, Missouri, USA and resulted in extensive building damage, 158 fatalities and over 1,000 injuries. The Joplin tornado is the costliest and the 7th deadliest tornado in U.S. history, with the maximum wind speed estimated to be more than 322 km hr^{-1} (200 mph). The track length was estimated at 35.6 km (22.1 miles), and the width was 1.2 km to 1.6 km ($3/4$ to 1 miles) (NWS 2011).

Six days after the Joplin tornado, a damage assessment team from the National Wind Institute (NWI) of Texas Tech University (TTU) was deployed. It spent four days traveling over 138 km within affected areas and recorded 14 hours of high-definition ground level video with two GPS-enabled video cameras for over 6,000 buildings.



- (a) Buildings (labeled with DOD) included in the ground survey across the tornado path as determined by the National Weather Service (NWS 2011)
- (b) A subset of Joplin damage swath (the region within the red square in (a)) and distribution of FR12 around the center line (blue line)

Fig. 1 Distribution of buildings from the post-tornado damage survey

The method of data collection and processing adopted in this study followed a similar methodology as previous studies done by the researchers from NWI (Brown *et al.* 2012, McMillan *et al.* 2008, Womble *et al.* 2006). Totally, there were 50,435 images extracted from the video, covering 6,579 buildings. Based on that, the wind damage states of all those buildings were manually assessed according to the Degree of Damage (DOD) in the EF scale (WISE 2006). Fig. 1 (a) shows the geographic distribution of the 6,579 buildings (labeled with DOD) included in the ground survey in the GIS database, along with the tornado path ratings determined by the National Weather Service (NWS).

For this study, a subset of Joplin tornado track was selected and 4,166 one- or two- family residences (FR12) buildings located in this area were used for the damage indicators and their DOD recorded, as shown in Fig. 1(b). There were two reasons to choose this subset. Firstly, in this region, the tornado reached its mature stage and made a large area of severe damage, Secondly, a huge amount of FR12 buildings in this area had been surveyed, which provided more stable and reliable measures of wind characters.

2.2 Wind speed estimation

Estimating wind speeds from the damage state of residence structures could be a complex process when structural design, construction material, and aging, previous exposure to severe events and duration of high winds, and other factors are considered. Therefore, the assumption was made that the damage of a building was primarily caused by the peak wind speed of tornado it experienced. In this way, the peak wind speed experienced by every FR12 was estimated from its DOD by using the corresponding expected wind speed in the EF scale, as shown in Table 1.

In the EF scale, there is no instruction on how to estimate the wind speed for an undamaged building, i.e., DOD=0, under the tornado wind environment. In this study, for buildings without any visual damage, the expected wind speed was set as 17.88 m s^{-1} (40 mph), which was estimated from wind speeds outside the damage area measured by the Joplin ASOS station (NIST 2013).

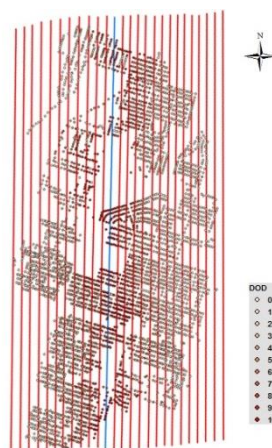


Fig. 2 Observed damage pattern (the map was rotated so that the tornado moved due north and bins were constructed from the center line (blue line) of tornado track at a 100 m interval)

Table 1 Degree of Damage (DOD) and associated wind speeds for one-and two-family residences (FR12) (WISE 2006)

DOD	Damage Description	Expected wind speed* (mph)	Lower bound wind speed* (mph)	Upper bound wind speed* (mph)
1	Threshold of visible damage	65	53	80
2	Loss of roof covering material (<20%), gutters and/or awning; loss of vinyl or metal siding	79	63	97
3	Broken glass in windows and doors	96	79	114
4	Uplift of roof deck and loss of significant roof covering material (>20%); collapse of chimney; garage doors collapse inward or outward; failure of porch or carport	97	81	116
5	Entire house shifts of foundation	121	103	141
6	Large sections of roof structure removed; most walls remain standing	122	104	142
7	Exterior walls collapse	132	113	153
8	Most walls collapsed in bottom floor, except small interior rooms	152	127	178
9	All walls collapsed	170	142	198
10	Destruction of engineered and/or well-constructed residence; slab swept clean	200	165	220

* The wind speeds shown in this table are 3-second gust speeds in mph

Due to the complex structure of a tornado, a significant degree of spatial variability in wind speed distribution should be expected. Therefore, a spatial averaging method was adopted to construct bins from the center line of the tornado track outward at a 100 m interval. To make a direct comparison between the peak wind speed profile estimated from the observations with the peak wind fields produced by the vortex simulations, the map (Fig. 1(b)) was rotated counterclockwise so that the tornado moved due north, as shown in Fig. 2. The average peak wind speed and the standard deviation in each bin were calculated. Those estimates were later used to calibrate parameters of the wind field model.

2.3 Vortex simulation and peak wind field reconstruction

A combined Rankine vortex model was used to simulate a steady tornado structure as shown in Eqs. (7)-(11). To simplify the model, it was assumed that the radius of maximum radial velocity is the same as the radius of maximum tangential velocity, i.e., $R_{\text{rmax}} = R_{\text{tmax}}$.

Then, to simulate the storm's forward motion, a translational velocity (V_s) was added to the radial and tangential velocity components. The peak wind field is constructed by recording the peak wind speeds at every grid point in the model.

In the translating Rankine vortex model, there were five main parameters, i.e., the radius of maximum radial/tangential velocity R_{max} , the maximum tangential wind velocity V_{tmax} , the maximum radial wind velocity V_{rmax} , the decay coefficient β and the translational velocity V_s . The

translational velocity of the tornado V_s was set as 11 m s^{-1} based on radar observation provided by the NWS (Karstens *et al.* 2013). The other four parameters were estimated based on the goodness-of-fit between the peak wind field model and observations.

An exhaustive search algorithm was designed to construct possible wind fields with different combinations of the above four parameters (R_{\max} , $V_{t\max}$, $V_{r\max}$, β). For each combination, a vortex model was run through the study area, which has both length and width of 3000 m, from grid point (0, -150) to grid point (0, 150) with a northern translational velocity 11 m s^{-1} . Meanwhile, the peak wind speed of every grid point was recorded and saved. In total, 408,000 peak wind fields were reconstructed.

To avoid under-sampling, the model used a grid spacing of 10 m and time step of 0.5 s, which was less than the threshold of time step given by Beck and Dotzek (2010) (Threshold = grid spacing/ $V_s = 10\text{m}/11\text{m s}^{-1} = 0.9 \text{ s}$).

2.4 Model fitting and selection

In this study, the observed and predicted peak wind speeds for each of bins were compared. Three indicators of goodness-of-fit were used for the selection of the best parameter estimation (i.e., the best fit model). They were coefficient of variation of the Root Mean Squared Deviation (CV(RMSD)), Pearson correlation coefficient (r), and the χ^2 goodness-of-fit test. RMSD measures the differences between the predicted values and the actual observed values, and is computed as the root of the mean of the squared deviation between actual observed values and values predicted by the fitted model. CV(RMSD) is a dimensionless number, which is defined as the ratio of the RMSD to the average of the observed values. It is calculated as follows

$$CV(RMSD) = \frac{RMSD}{\bar{o}} = \frac{\sqrt{\frac{\sum_{i=1}^k (m_i - o_i)^2}{k}}}{\bar{o}} \quad (12)$$

where m_i is the model mean for bin i , o_i is the observed mean for each bin i , k is the total number of bins, and \bar{o} is the mean of the observed values.

Pearson correlation coefficient reflects the strength of a linear relationship and thus measures the similarity in relative trend magnitudes of the observed data and the fitted model. The χ^2 goodness-of-fit tests the null hypothesis that the observed data are consistent with the model distribution.

The best-fit model is the one with a smaller CV(RMSD), higher r , and the one for which χ^2 goodness-of-fit test fails to reject the null hypothesis (Schunn and Wallach 2005).

3. Results

Fig. 3 shows a reasonable agreement between the peak wind speed profile produced by the best-fit model and those estimated from observed building damage. It has the smallest CV(RMSD) (0.06) among 408,000 possible cases and a relatively higher r (0.99). In addition, for the χ^2 goodness-of-fit test, the null hypothesis failed to be rejected with p-value great than the 5% significant level.

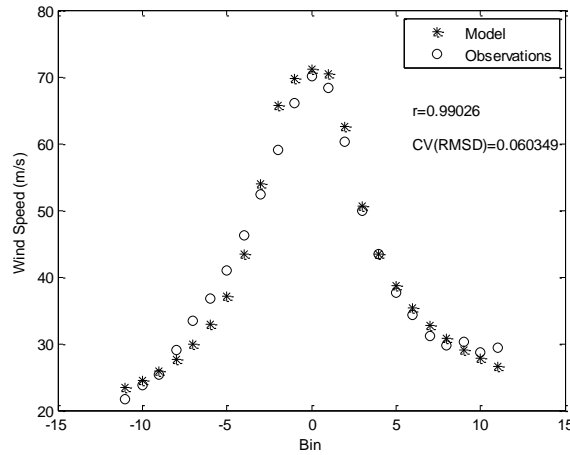
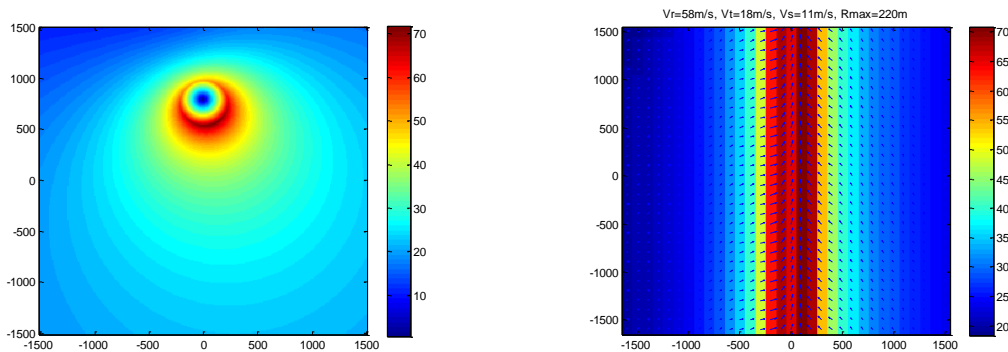


Fig. 3 Comparison of peak wind speeds between the best-fit model and the post-tornado damage survey

In this best-fit model, the core radius R_{max} is estimated to be 220 m, the maximum tangential wind velocity V_{tmax} is estimated to be 18 m s^{-1} , the maximum radial wind velocity V_{rmax} is estimated to be 58 m s^{-1} , and the decay coefficient β is estimated to be 0.7. Fig. 4(a) shows an example of the instantaneous wind field obtained from a translating Rankine vortex with those parameters, and Fig. 4(b) shows the peak wind field from the best-fit model with peak wind speed and direction on a 100 m by 100 m grid. It is noteworthy that the maximum wind speed is offset from the center line due to the effects of translation which increased the wind speeds on the right side and decreased the wind speeds on the left side of the vortex center by adding a northern uniform translational component to the radial and tangential velocity components of the vortex.



(a) An example of the instantaneous wind field obtained from a translating Rankine vortex (b) The peak wind field from the best-fit model

Fig. 4 Wind field simulation from a Rankine vortex model with a northern uniform component

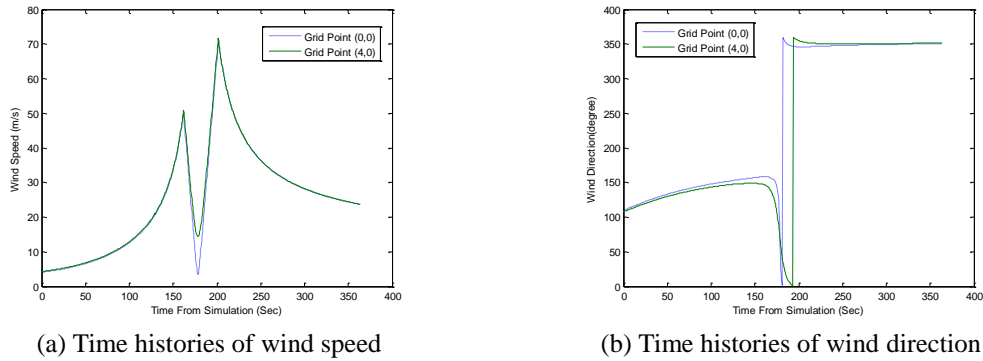


Fig. 5 Time histories of wind speeds and directions of (0,0) and (4,0) from the best-fit model

Furthermore, two points were selected as examples to illustrate time history of wind speed and direction. The first one, grid point (0, 0), is located in the center of the study area and would be the tornado eye if there is no translational velocity. The second one, grid point (4, 0), is where the peak wind speed has the maximum value among all the points on the same horizontal line. The time histories of wind speeds and directions of those two points are shown in Fig. 5. Both points contain two wind speed peaks about 40 seconds apart as well as one sharp drop in wind speeds between these two peaks that corresponds to the arrival and passing of the tornado eye. Meanwhile, wind direction also changed dramatically as the tornado eye is approaching and leaving (the wind direction was measured clockwise from north).

4. Discussion

This study attempts to reconstruct the near-surface wind field based on building damage states observed from a field survey in Joplin after the 2011 EF 5 tornado. It's found that the peak wind field produced by a simplified translating analytical vortex model agrees reasonably well with the observed damaged pattern, suggesting the validity of the method being used.

By matching observed tree damage patterns with simulated forest damage, Karstens *et al.* (2013) and NIST (2013) reconstructed the near-surface wind field of the Joplin tornado separately. One difference between these two studies is their adopted tree-fall models; the other is about their methods to find the best matched model, i.e., NIST (2013) used full factorial design, main- and interaction-effects plots to determine the effects of input parameters' variation on output parameters and narrow the ranges of parameters, whereas Karstens *et al.* (2013) relied on subjective evaluation to match the observed tree-fall pattern with simulated patterns.

Table 2 shows the comparison of parameters and outputs estimated by those three translating Rankine vortices in the best-fitting models.

For the best-fit model, the core radius was estimated to be 220 m by this study, closer to the estimate of NIST (2013), but much smaller than the subjective estimate from the remote sensing imagery by Karstens *et al.* (2013). Comparing to Karstens *et al.* (2013), the values of wind velocity components V_{tmax} and V_{rmax} in this study are smaller. NIST (2013) didn't report its V_{tmax} and V_{rmax} but presented the values of α and G_{max} , which was related to V_{tmax} , V_{rmax} and V_s . Given the

values of these parameters, the values of α and G_{\max} could then be calculated for Karstens *et al.* (2013) as well as this study. It shows that the values of this study are relatively consistent with the values reported by NIST (2013). For the decay coefficient β , Karstens *et al.* (2013) adopted the model with $\beta=1$, whereas the value estimated by NIST (2013) was between 0.6 and 0.7 from the effect analysis, which is consistent with the 0.7 of this study. Finally, Karstens *et al.* (2013) presented a highest maximum wind speed, whereas the other two studies reached smaller expected maximum wind speed with uncertainty ranges.

The relatively large discrepancy in the maximum wind speed estimates of those three studies is possibly associated with the different methods in searching for the best-fit model. Karstens *et al.* (2013) chose their best-fit model by subjectively evaluating the similarity between the simulated and observed tree-fall patterns. The accuracy of subjective evaluation is always a concern because of potential biases introduced by individuals who conduct the evaluation. In contrast, this study uses statistical methods and thus minimizes the potential human biases associated with manually selecting and evaluating model parameters. Furthermore, Karstens *et al.* (2013) only presented one value of the maximum wind speed, whereas NIST (2013) and this study estimated intervals for the maximum wind speed, which are more desirable than a single value because they take into consideration uncertainties of tornado wind field caused by factors such as complex topographic effects and climate conditions. In addition, the estimated maximum wind speed from Karsten *et al.* (2013) fell in the range of EF 5 tornado, whereas the expected maximum wind speeds from NIST (2013) and this study are less than the lower bound of EF 5, which seem to underestimate the event. However, a closer emanation showed that this was not the case. Actually, according to the EF scale (WISE 2006), the intensity of a tornado event is rated based on the highest rated DIs found in the damage area. It means that within an EF 5 tornado track, some areas could be rated as EF 5 and others may be rated with less intensity. Fig. 4(b) shows clearly that even for the bin that is closest to the central line, only some buildings experienced the degree of damage that corresponded to EF 5 wind force due to randomness intrinsic in the tornado process. Therefore, the average EF scale for that bin is lower than EF 5. Since both intervals estimated by NIST (2013) and this study partially overlapped with the range of EF 5 wind speeds, the fact that the expected maximum wind speeds from those two studies did not reach EF 5 just reflects that EF scale is rated based only on the highest rated DI in the damage area.

Table 2 Comparison of parameters and outputs of the best-fit models for the 2011 Joplin Tornado

	Karstens <i>et al.</i> (2013)	NIST (2013)	This Study
RMW (m)	300.00	258.00	220.00
V_{tmax} (m s^{-1})	43.00	-	18.00
V_{rmax} (m s^{-1})	86.00	-	58.00
α (degree)*	26.57	15.00 - 25.00	17.24
G_{\max} *	8.74	4.50 - 5.00	5.52
β	1.00	0.60 - 0.70	0.70
Maximum wind speed (m s^{-1})	104	78.23 ± 15.65	71.18 ± 22.72

* α is the angle between the radial velocity and the circular velocity, the latter is the vector sum of the radial velocity and the tangential velocity; G_{\max} is the ratio between the maximum circular velocity and the translational velocity (NIST 2013)

One advantage of using building damages to reconstruct the near-surface wind field is that buildings usually are less vulnerable to wind than other DIs are and thus can indicate higher wind speeds. For example, among all DIs used by the EF scale, the one- or two-family residence (FR12) is one of those that can indicate the highest expected wind speed (89.41 m s^{-1}). Other DIs, like the tree used by previous studies, can only indicate expected wind speed as high as 62.59 m s^{-1} . Consequently, buildings are more suitable for reconstruction of violent tornado wind field than other DIs. Furthermore, buildings are places where people live and work. The damages to buildings carry more direct social and economic consequences and thus attracted wide public attention and research interests. Accordingly, the study of wind field in the area of buildings is more important and presents greater opportunities to understand how natural hazards interact with built environment and eventually affect the resilience to hazards. Moreover, since many more studies have been conducted about buildings than trees, there is greater potential to applying the latest findings on the relationship of building damage and wind speed to refine wind fields.

Some limitations should be noted along with the contributions. Comprehensive sensitivity analysis has yet to be conducted to ensure that parameters were robust and not sensitive to different estimations of damage. Furthermore, in this study, only one factor (i.e., the peak wind speed) was considered in the model for causing building damage while in fact during the time histories of tornado wind speed and direction, the effect of rapid changes in wind speed and direction, surrounding buildings, surface roughness, and building attributes (e.g., quality, orientation, style, and building material), etc. are known to affect wind loading and structural performance (Haan *et al.* 2010, Kopp and Morrison 2010, Lewellen and Zimmerman 2008, Zhang and Sarkar, 2009). While those factors are not modeled separately, their influences could be implicitly captured by the uncertainty in wind speed estimation as the peak wind speed is deemed as the dominant factor.

Relationships between DODs and wind speeds in the EF scale is important to the findings of this study and could affect the accuracy of wind speed estimation. Two sources of biases may be introduced during the wind speed estimation.

One is related to the development of EF scale. According to the EF scale report (WISE 2006), the estimation of wind speeds associated with DODs is based on expert elicitation. It is a subjective evaluation of wind speeds (Mehta 2013). There are two major problems with this method. Firstly, as mentioned above, wind speed is only one of the many factors that cause the structure damage and EF scale integrates all the factors into a single factor (i.e., peak wind speed). Consequently, the estimated wind speeds from expert elicitation may deviate from the actual wind speeds. Secondly, since direct and reliable measurements of near ground tornado wind speed were rare at the time when the report was delivered, experts' elicitation was very likely to be based on their experiences on wind damage from straight-line winds or hurricanes, which have different mechanisms of wind loads from those of tornadoes (Haan *et al.* 2010, Simiu and Scanlan 1996). Thus, more credible and reliable estimation of the wind speed is desired.

The second source of biases appears in the practical use of EF scale. Investigators do not always agree with each other on the level of DOD for the same building because of their differences in experiences, backgrounds, and study focus etc. (Edwards *et al.* 2013, NIST 2013). In addition, the quality of buildings affects the relationship between DOD and wind speeds, which is addressed by EF scale with a range of wind speeds for each DOD, i.e., low bound, expected, and upper bound of estimated wind speeds. However, for this particular study, only the expected wind speed for a certain DOD is used because of the lack of access to information of building quality.

5. Conclusions

The post-tornado survey of buildings can provide the most accurate information on the degree of damage, which has direct connection with the wind speed those buildings experienced. Particularly when radar observations cannot measure wind lower than 20 – 30 m AGL, this method can advance our knowledge about near-surface wind field.

In spite of its simplicity, the analytical method developed in this study can produce a reasonable estimation of the near-surface wind field consistent with the degree of damage of buildings observed from a post-tornado damage survey. The resulting model not only helps better understand the dynamics of near-surface tornado structure on both temporal and spatial scales, but also provides useful information for engineering and safety purposes. Furthermore, findings from this study can also be incorporated in catastrophe modelling of future tornado risks on the built environment and public health. Overall, the methods and findings of this study will contribute to emergency management, building codes, and insurance and risk modeling.

It is noteworthy that the major purpose of this study is to examine how post-tornado damage surveys could be better used to reconstruct near-surface wind field. Thus, only a subset of an EF 5 tornado with relatively homogenous characteristics was modeled. In the future, this study could be expanded to examine the effectiveness of this method when applied to other types of tornadoes (e.g., larger, smaller, strong, or weaker tornadoes). More data could be collected and analyzed, resulting in generalized models for tornadoes with varied intensities and other attributions.

One area of future work is to explore the use of remote-sensing based damage survey to reconstruct the near-surface wind field. A limitation about the post-tornado ground-based damage survey is that it could only cover those buildings that could be accessible at the time of data collection and would miss the buildings where the roads were damaged or blocked. Therefore, bias is always a concern because a representative sample is hard to reach. Moreover, ground-based survey is always time-consuming and expensive to carry out. Remote-sensing based damage survey could address those problems. It could be a rapid way to reconstruct the wind field after the relationship of remote-sensing damage scale and ground level damage scale is well studied (Brown *et al.* 2012, Luo *et al.* 2014).

Another area of future research involves the wind speed estimation from DODs in the EF scale. In this case, methods of wind speed estimation that are relatively more objective than expert elicitation are needed to validate and establish the credibility and reliability of the EF scale wind speeds. To find the relationships between tornado wind speeds and DODs of buildings, one method mentioned by the EF scale report (but not adopted due to time and budget limitations) is to use a load/resistance approach to estimate damage to a structure (WISE 2006). Furthermore, simulations could be used to establish more reliable statistical relationships between building damage states and wind speeds. This is also the methodology adopted by HAZUS-MH Hurricane (Vickery *et al.* 2006). This method relies on a great deal of laboratory test data and involves many assumptions to build idealized models for limited types of structures. Another method is to combine in situ observations or mobile Doppler radar measurement with traditional damage-based survey. In situ observations and mobile radar, particularly those that transmit at a high frequency (e.g., the Texas Tech Ka-band radars), could be used to measure wind and reconstruct wind field. Field surveys could provide DOD of buildings within the study area. Then the relationships between wind speeds and damage states of buildings could be established. Through a large number of observations combining various damage states and wind speeds, the interactions of complex wind fields in space and time with different characteristics of structures would be observed and the

uncertainties in structures and tornadoes can be addressed. With statistical models, the relationships between wind speeds and DOD of buildings could be better estimated by controlling other factors that influence the damage.

Acknowledgements

This material is partially based upon work in part supported by the National Science Foundation under Grants CMMI-1000251 and 1131392. Any opinions, findings, and conclusions or recommendations expressed in this paper are those of the authors and do not necessarily reflect the views of the National Science Foundation.

References

- Bech, J., Gayà, M., Aran, M., Figuerola, F., Amaro, J. and Arús, J. (2009), "Tornado damage analysis of a forest area using site survey observations, radar data and a simple analytical vortex model", *Atmos. Res.*, **93**(1), 118-130.
- Beck, V. and Dotzek, N. (2010), "Reconstruction of near-surface tornado wind fields from forest damage", *J. Appl. Meteorol. Climatol.*, **49**(7), 1517-1537.
- Bluestein, H.B., Pazmany, A.L., Galloway, J.C. and McIntosh, R.E. (1995), "Studies of the substructure of severe convective storms using a mobile 3-mm-wavelength Doppler radar", *B. Am. Meteorol. Soc.*, **76**(11), 2155-2169.
- Bluestein, H.B., Weiss, C.C. and Pazmany, A.L. (2003), "Mobile Doppler radar observations of a tornado in a supercell near Bassett, Nebraska, on 5 June 1999. Part I: Tornadogenesis", *Mon. Weather Rev.*, **131**(12), 2954-2967.
- Brown, R.A. and Wood, V.T. (1991), "On the interpretation of single-Doppler velocity patterns within severe thunderstorms", *Weather Forecast.*, **6**(1), 32-48.
- Brown, T.M., Liang, D. and Womble, J.A. (2012), "Predicting ground-based damage states from windstorms using remote-sensing imagery", *Wind Struct.*, **15**(5), 369-383.
- Burgers, J.M. (1948), "A mathematical model illustrating the theory of turbulence", *Adv. Appl. Mech.*, **1**, 171-199.
- Burgess, D.W., Magsig, M.A., Wurman, J., Dowell, D.C. and Richardson, Y. (2002), "Radar observations of the 3 May 1999 Oklahoma City tornado", *Weather Forecast.*, **17**(3), 456-471.
- Davies-Jones, R., Trapp, R.J. and Bluestein, H.B. (2001), "Tornadoes and tornadic storms", *Severe Convective Storms, Meteor. Monogr.*, **28**, 167-221.
- Doswell III, C.A., Brooks, H.E. and Dotzek, N. (2009), "On the implementation of the enhanced Fujita scale in the USA", *Atmos. Res.*, **93**(1-3), 554-563.
- Doswell III, C.A. and Burgess, D.W. (1993), "Tornadoes and tornadic storms: A review of conceptual models", *Geophys. Monogr. Ser.*, **79**, 161-172.
- Edwards, R., LaDue, J.G., Ferree, J.T., Scharfenberg, K., Maier, C. and Coulbourne, W.L. (2013), "Tornado Intensity Estimation: Past, Present, and Future", *B. Am. Meteorol. Soc.*, **94** (5), 641-653.
- Fujita, T.T. (1971), *Proposed Characterization of Tornadoes and Hurricanes by Area and Intensity*, University of Chicago, Chicago, Illinois, USA.
- Fujita, T.T. (1981), "Tornadoes and downbursts in the context of generalized planetary scales", *J. Atmos. Sci.*, **38**(8), 1511-1534.
- Haan, F.L., Jr., Balaramudu, V.K. and Sarkar, P.P. (2010), "Tornado-induced wind loads on a low-rise building", *J. Struct. Eng. - ASCE*, **136**(1), 106-116.
- Holland, A.P., Riordan, A.J. and Franklin, E.C. (2006), "A simple model for simulating tornado damage in

- forests”, *J. Appl. Meteorol. Climatol.*, **45**(12), 1597-1611.
- Karstens, C.D., Gallus Jr, W.A., Lee, B.D. and Finley, C.A. (2013), “Analysis of Tornado-Induced Tree-Fall Using Aerial Photography from the Joplin, MO, and Tuscaloosa-Birmingham, AL, Tornadoes of 2011”, *J. Appl. Meteorol. Climatol.*, **52**(5), 1049-1068.
- Karstens, C.D., Samaras, T.M., Lee, B.D., Gallus Jr, W.A. and Finley, C.A. (2010), “Near-Ground Pressure and Wind Measurements in Tornadoes”, *Mon. Weather Rev.*, **138**(7), 2570-2588.
- Kopp, G.A. and Morrison, M.J. (2010), “Discussion of “Tornado-Induced Wind Loads on a Low-Rise Building” by F. L. Haan Jr., Vasanth Kumar Balaramudu, and P. P. Sarkar”, *J. Struct. Eng. - ASCE*, **137**(12), 1620-1622.
- Kosiba, K. and Wurman, J. (2010), “The three-dimensional axisymmetric wind field structure of the Spencer, South Dakota, 1998 tornado”, *J. Atmos. Sci.*, **67**(9), 3074-3083.
- Kosiba, K.A., Trapp, R.J. and Wurman, J. (2008), “An analysis of the axisymmetric three-dimensional low level wind field in a tornado using mobile radar observations”, *Geophys. Res. Lett.*, **35**(5), L05805.
- Lee, W.C. and Wurman, J. (2005), “Diagnosed three-dimensional axisymmetric structure of the Mulhall tornado on 3 May 1999”, *J. Atmos. Sci.*, **62**(7), 2373-2393.
- Lewellen, D.C. and Lewellen, W.S. (2007), “Near-surface intensification of tornado vortices”, *J. Atmos. Sci.*, **64**(7), 2176-2194.
- Lewellen, D.C. and Zimmerman, M.I. (2008), “Using simulated tornado surface marks to help decipher near-ground wind fields”, *Preprints, 24th Conf. on Severe Local Storms, Amer. Meteor. Soc. B*, Savannah, GA, USA.
- Luo, J., Liang, D., Kafali, C., Li, R. and Brown, T. M. (2014), “Enhanced remote-sensing scale for wind damage assessment”, *Wind Struct.*, **19**(3), 321-327
- Mallen, K.J., Montgomery, M.T. and Wang, B. (2005), “Reexamining the near-core radial structure of the tropical cyclone primary circulation: Implications for vortex resiliency”, *J. Atmospheric Sci.*, **62**(2), 408-425.
- McMillan, A., Adams, B. J., Reynolds, A., Brown, T., Liang, D., and Womble, J. A. (2008), “Advanced technology for rapid tornado damage assessment following the ‘Super Tuesday’ tornado outbreak of February 2008”, MCEER Report, University of Buffalo, Buffalo, NY.
- Mehta, K.C. (2013), “Development of the EF-Scale for Tornado Intensity”, *J. Disaster Res.*, **8**(6), 1034-1041.
- NIST (2013), *Technical Investigation of the May 22, 2011, Tornado in Joplin, Missouri*, National Institute of Standards and Technology, Gaithersburg, MD, USA.
- NWS (2011), “Joplin Tornado Event Summary - May 22, 2011”, <http://www.crh.noaa.gov/sgf/?n=event_2011may22_summary> (accessed September 21, 2013).
- Peterson, R.E. (1992), “Johannes Letzmann: A pioneer in the study of tornadoes”, *Weather Forecast.*, **7**(1), 166-184.
- Potvin, C.K., Shapiro, A., Yu, T.Y., Gao, J. and Xue, M., (2009), “Using a Low-Order Model to Detect and Characterize Tornadoes in Multiple-Doppler Radar Data”, *Mon. Weather Rev.*, **137**(4), 1230-1249.
- Rankine, W.J.M. (1882), *A Manual of Applied Mechanics*, (10th Ed.), Charles Griffin and Company, London, UK.
- Rott, N. (1958), “On the viscous core of a line vortex”, *Z. Für Angew. Math. Phys. ZAMP*, **9**(5-6), 543-553.
- Schunn, C.D. and Wallach, D. (2005), “Evaluating goodness-of-fit in comparison of models to data”, (Ed. W. Tack), *Psychologie Der Kognition: Reden and Vorträge Anlässlich Der Emeritierung von Werner Tack*, University of Saarland Press, Saarbrücken, Germany.
- Simiu, E. and Scanlan, R.H. (1996), *Wind Effects on Structures: Fundamentals and Applications to Design*, (3rd Ed.), John Wiley, New York, USA.
- Sullivan, R.D. (1959), “A Two-Cell Vortex Solution of the Navier-Stokes Equations”, *J. Aerosp. Sci.*, **26**(11), 767-768.
- Tanamachi, R.L., Bluestein, H.B., Lee, W.C., Bell, M. and Pazmany, A. (2007), “Ground-based velocity track display (GBVTD) analysis of W-band Doppler radar data in a tornado near Stockton, Kansas, on 15 May 1999”, *Mon. Weather Rev.*, **135**(3), 783-800.

- Toth, M., Trapp, R.J., Wurman, J. and Kosiba, K.A. (2013), "Comparison of Mobile-Radar Measurements of Tornado Intensity with Corresponding WSR-88D Measurements", *Weather Forecast.*, **28**(2), 418-426.
- Vickery, P.J., Skerlj, P.F., Lin, J., Twisdale Jr, L.A., Young, M.A. and Lavelle, F.M. (2006), "HAZUS-MH hurricane model methodology. II: Damage and loss estimation", *Nat. Hazards Rev.*, **7**, 94-103.
- WISE (2006), *A Recommendation for an Enhanced Fujita Scale (EF-Scale)*, Wind Science and Engineering Research Center, Texas Tech University, Lubbock, Texas, USA.
- Wood, V.T. and Brown, R.A. (2011), "Simulated tornadic vortex signatures of tornado-like vortices having one-and two-celled structures", *J. Appl. Meteorol. Climatol.*, **50**(11), 2338-2342.
- Wood, V.T. and White, L.W. (2011), "A new parametric model of vortex tangential-wind profiles: Development, testing, and verification", *J. Atmos. Sci.*, **68**(5), 990-1006.
- Womble, J.A., Ghosh, S., Adams, B.J. and Friedland, C.J. (2006), *Advanced Damage Detection for Hurricane Katrina: Integrated Remote Sensing & VIEWS TM Field Reconnaissance*, MCEER Report, University of Buffalo, Buffalo, NY, USA.
- Wurman, J. and Alexander, C.R. (2005), "The 30 May 1998 Spencer, South Dakota, storm. Part II: comparison of observed damage and radar-derived winds in the tornadoes", *Mon. Weather Rev.*, **133**(1), 97-119.
- Wurman, J. and Gill, S. (2000), "Finescale radar observations of the Dimmitt, Texas (2 June 1995), tornado", *Mon. Weather Rev.*, **128**(7), 2135-2164.
- Wurman, J., Kosiba, K., Markowski, P., Richardson, Y., Dowell, D. and Robinson, P. (2010), "Finescale single-and dual-doppler analysis of tornado intensification, maintenance, and dissipation in the orleans, nebraska, supercell", *Mon. Weather Rev.*, **138**(12), 4439-4455.
- Wurman, J., Kosiba, K. and Robinson, P. (2013), "In Situ, Doppler Radar, and Video Observations of the Interior Structure of a Tornado and the Wind-Damage Relationship", *B. Am. Meteorol. Soc.*, **94**(6), 835-846.
- Wurman, J., Robinson, P., Alexander, C. and Richardson, Y. (2007), "Low-level winds in tornadoes and potential catastrophic tornado impacts in urban areas", *B. Am. Meteorol. Soc.*, **88**(1), 31-46.
- Wurman, J., Straka, J., Rasmussen, E., Randall, M. and Zahrai, A. (1997), "Design and deployment of a portable, pencil-beam, pulsed, 3-cm Doppler radar", *J. Atmos. Ocean. Tech.*, **14**(6), 1502-1512.
- Zhang, W. and Sarkar, P.P. (2009), "Influence of surrounding buildings on tornado-induced wind loads of a low-rise building", *Proceedings of the 11th American Conference on Wind Engineering*, San Juan, Puerto Rico, USA.
- Zrnic, D., Burgess, D.W. and Hennington, L. (1985), "Doppler spectra and estimated windspeed of a violent tornado", *J. Clim. Appl. Meteorol.*, **24**(10), 1068-1081.